Communication

Orientation Control of Fluorescence Resonance Energy Transfer Using DNA as a Helical Scaffold

Frederick D. Lewis, Ligang Zhang, and Xiaobing Zuo

J. Am. Chem. Soc., **2005**, 127 (28), 10002-10003• DOI: 10.1021/ja0524402 • Publication Date (Web): 21 June 2005

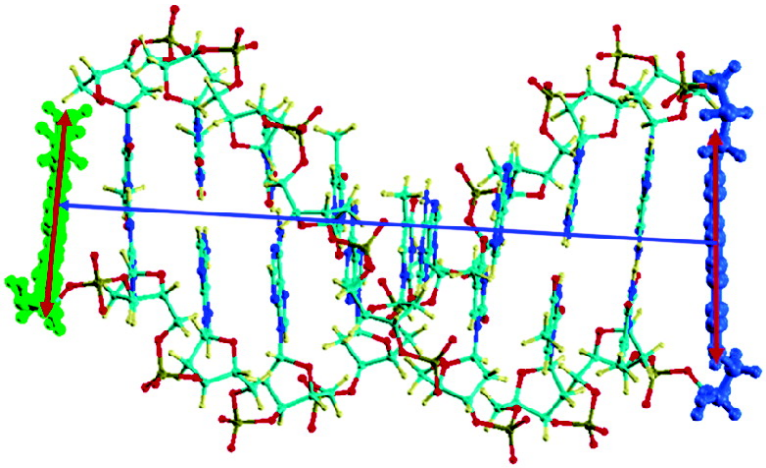

J|A|C|S
COMMUNICATIONS

Published on Web 06/21/2005

Orientation Control of Fluorescence Resonance Energy Transfer Using DNA as a Helical Scaffold

Frederick D. Lewis,*,† Ligang Zhang,† and Xiaobing Zuo‡

Department of Chemistry, Northwestern University, Evanston, Illinois 60208, and Chemistry Division, Argonne National Laboratory, Argonne, Illinois 60439

Received April 14, 2005; E-mail: lewis@chem.northwestern.edu

Fluorescence resonance energy transfer (FRET) between an excited fluorescence donor and a ground state fluorescence acceptor has been widely used to study the structure and dynamics of molecules in the gas phase, solution, and solid state.[1,2] FRET has been employed in studies of DNA duplex formation, duplex structure, and duplex protein binding. Elegant studies by Clegg et al.[3,4] and by Hurley and Tor[5] using complementary duplexes possessing donor and acceptor probes separated by a variable number of base pairs have shown that the FRET efficiency is dependent upon the vector distance between the chromophores, rather than the number of base pairs. Jovin employed an ingenious FRET experiment to establish the helical handedness of short duplexes.[6]

According to the semiclassical vector model proposed by Förster, the efficiency, E, of FRET can be described by eq 1, where R_{DA} is the distance between the fluorescence donor and acceptor, and R_o is the distance (Å) at which half of the energy is transferred (the Förster radius).[2,3]

$$E = R_o^6/[R_o^6 + R_{DA}^6] \quad (1)$$

$$R_o = 0.2108[J_{DA}(\lambda)\kappa^2 n^{-4}\Phi_D]^{1/6} \quad (2)$$

$$\kappa = \vec{e}_1\cdot\vec{e}_2 - 3(\vec{e}_1\cdot\vec{e}_{12})(\vec{e}_{12}\cdot\vec{e}_2) \quad (3)$$

The value of R_o is described by eq 2, where $J(\lambda)$ is the donor/acceptor spectral overlap integral, κ is a geometric factor associated with the orientation of the donor and acceptor dipoles, and n is the refractive index of the medium separating the donor and acceptor. The value of κ is described by eq 3, where e_1, e_2, and e_{12} are the unit vectors of the donor and acceptor transition dipoles and distance between their centers. Whereas the distance dependence of FRET has been extensively documented, the orientation dependence has been observed only for a small number of systems having fixed donor−acceptor orientation.[7] We report here the efficiency of FRET for a series of DNA conjugates in which a stilbene dicarboxamide (SA, donor) and perylenedicarboxamide (PA, acceptor) are covalently attached to opposite ends of an A:T base pair duplex domain consisting of 4−12 base pairs. The results demonstrate for the first time the systematic dependence of FRET efficiency upon the orientation factor, thus confirming the orientation dependence predicted by Förster theory.

Capped hairpin conjugates SA−PA$_N$ possessing a SA hairpin linker and PA end cap at opposite ends of a base pair domain consisting of N A:T base pairs (Figure 1a) were prepared and characterized as described in Supporting Information (SI), using procedures previously employed for capped hairpins with stilbene chromophores at both ends of the base pair domains.[8] The high melting temperature and well-developed CD spectra of SA−PA$_4$ (SI) are indicative of the formation of a compact folded structure in which PA is π-stacked with the adjacent base pair. Poly(dA)−poly(dT) base pair domains, known as A-tracts or B′-DNA, were selected based on their regular helical structures.[9]

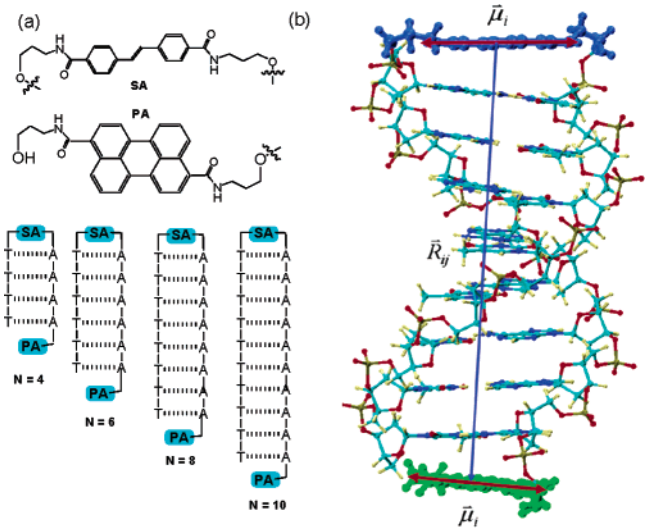

Figure 1. (a) Formulas for the SA linker and PA end cap and two-dimensional models of SA−PA$_N$ conjugates. N is the number of A:T base pairs separating the chromophores. (b) Side view of a molecular model for conjugate SA−PA$_8$. The SA and PA linkers are located at the top and bottom, respectively, of a B-DNA base pair domain. Vectors indicate the chromophore electronic transition dipoles and the center-to-center distance. The SA and PA vectors are fixed relative to long axes of the adjacent base pairs at angles of 17 and 0°, respectively.

The absorption and fluorescence emission spectra of the isolated SA and PA chromophores are shown in Figure 2a. The SA chromophore can be selectively excited at 337 nm, at which wavelength PA has weak absorbance. The SA fluorescence spectrum overlaps with the PA absorption spectrum, with a calculated overlap integral $J_{DA} = 3.0 \times 10^{14}$. Thus SA serves as the singlet energy donor and PA as the acceptor.

The fluorescence spectra of the SA−PA$_N$ conjugates are shown in Figure 2b. Quantum yield (Φ_f) and lifetime (τ) data for SA are shown in Figure 3a,b (tabular data provided in SI). The values of Φ_f and τ_D for SA increase as the number of base pairs, N, separating SA and PA increases, reaching values for $N = 12$ comparable to those for SA-linked hairpins lacking the PA acceptor ($\Phi_f = 0.35$ and $\tau = 2.1$ ns).[10] However, the increases are not continuous with N. The values of Φ_f for PA display an inverse correlation with those for SA, decreasing in noncontinuous fashion as Φ_f for SA increases. The values of τ for PA are the same as that of a PA-linked hairpin (6.5 ± 0.1 ns) and are independent of the length of the base pair domain, as expected for an irreversible energy transfer process.

† Northwestern University.
‡ Argonne National Laboratory.

10.1021/ja0524402 CCC: $30.25

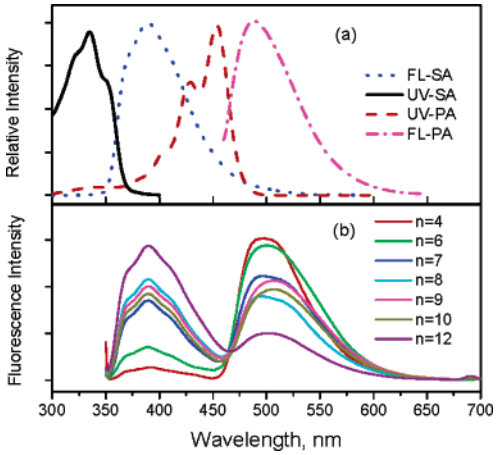

Figure 2. (a) Ultraviolet (UV) absorption and fluorescence (FL) spectra of the diol derivatives of SA and PA (2×10^{-6} M, see Figure 1 for structures) in methanol solution. (b) Fluorescence spectra of SA−PA_N capped hairpins in aqueous buffer (1.5×10^{-6} M, 10 mM phosphate, pH 7.2, 100 mM NaCl). Excitation wavelength = 337 nm.

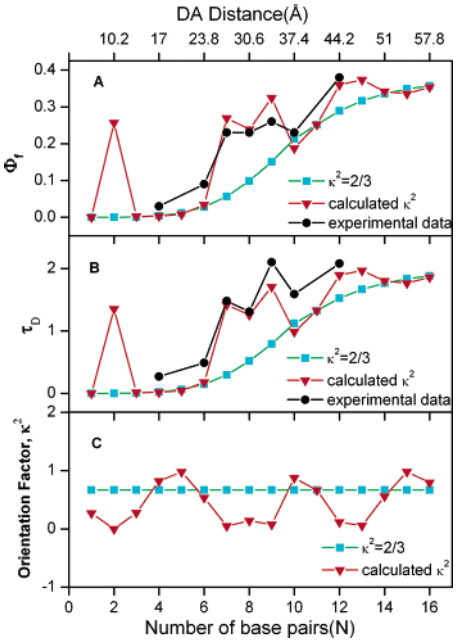

Figure 3. (a) Quantum yields (estimated error ±10%) and (b) lifetimes (estimated error ±5−15%) for SA fluorescence from SA−PA_N conjugates. These values can be used to determine the efficiency of quenching (eq 1) from the equations $\tau_D = \tau_D^\circ (1 - E)$ and $\Phi_f = \Phi_f^\circ(1 - E)$. (c) Values of κ^2 as a function of N and calculated distance.

A dipole vector model for conjugate SA−PA_8 is shown in Figure 1b. The SA and PA transition moments are assumed to be long-axis polarized, as is the case for the parent stilbene and perylene chromophores.[11] The model is constructed using B-DNA geometry, which has a slightly larger helical pitch than does an A-tract (36° versus 34°). The 17° vector angle for the SA linker is based on the crystal structure of a stilbene-linked hairpin,[12] whereas the angle for the PA linker (0°) was adjusted to obtain agreement between calculated and experimental data. Values of κ^2 calculated using this structural model are shown in Figure 3c along with the value of $\kappa^2 = {}^2/_3$, which is conventionally assumed for randomly oriented dipoles.[2] Small changes in the interchromophore angle (±10°) have little effect on the calculated values of κ^2.

Calculated values for the SA quantum yield and lifetime obtained using the oriented dipole model and using a constant value of $\kappa^2 = {}^2/_3$ are shown in Figure 3a,b, along with the experimental data. The experimental values are seen to be in good agreement with the values obtained using the oriented dipole model, but not with those provided by the averaged dipole model. Agreement with the oriented dipole model requires that the PA dipole be aligned with the duplex (as observed for SA-capped hairpins[8]) and not randomly oriented. The discrepancy between the experimental data and averaged dipole model is particularly noticeable for $N = 7-9$, the observed singlet lifetime being as much as 5 times longer than the singlet lifetime predicted by the averaged dipole model. The oriented dipole model predicts near-zero values of κ^2 for these conjugates (Figure 3c), in accord with the inefficient quenching of the SA donor fluorescence quantum yields and lifetimes.

To summarize, the use of A-tract DNA base pair domains as a helical scaffold has permitted the first systematic study of the effect of chromophore orientation upon FRET efficiency. The effect of orientation is most pronounced at distances near the Förster radius (33 Å, as calculated using $\kappa^2 = {}^2/_3$). At shorter distances, rapid electron exchange (Dexter) quenching may preclude observation of the local maximum in Φ_f and τ_D predicted for $N = 2$ (Figure 3).[13] Since the Förster radius is determined by the spectral overlap integral and the donor quantum yield (eq 2), it should be possible to design capped hairpin systems with either shorter or longer Förster radii. Such systems may provide sensitive probes of DNA conformational changes which occur upon intercalation or binding of small molecules or proteins.

Acknowledgment. This research is supported by the Division of Chemical Sciences, Office of Basic Energy Sciences, U.S. Department of Energy under Contract DE-FG02-96ER14604.

Supporting Information Available: Preparation of PA, CD spectra, and quantum yield and lifetime data. This material is available free of charge via the Internet at http://pubs.acs.org.

References

(1) (a) Stryer, L. *Annu. Rev. Biochem.* **1978**, *47*, 819−846. (b) Selvin, P. R. *Nat. Struct. Biol.* **2000**, *7*, 730−734.
(2) Lakowwicz, J. R. *Principles of Fluorescence Spectroscopy*, 2nd ed.; Kluwer Academic: New York, 1999.
(3) Clegg, R. M. *Methods Enzymol.* **1992**, *211*, 353−388.
(4) Clegg, R. M.; Murchie, A. I. H.; Zechel, A.; Lilley, D. M. J. *Proc. Natl. Acad. Sci. U.S.A.* **1993**, *90*, 2994−2998.
(5) Hurley, D. J.; Tor, Y. *J. Am. Chem. Soc.* **2002**, *124*, 13231−13241.
(6) Jares-Erijman, E. A.; Jovin, T. M. *J. Mol. Biol.* **1996**, *257*, 597−617.
(7) (a) Maus, M.; De, R.; Lor, M.; Weil, T.; Mitra, S.; Wiesler, U.-M.; Herrmann, A.; Hofkens, J.; Vosch, T.; Mullen, K.; De Schryver, F. C. *J. Am. Chem. Soc.* **2001**, *123*, 7668−7676. (b) Hübner, C. G.; Ksenofontov, V.; Nolde, F.; Müllen, K.; Basché, T. *J. Chem. Phys.* **2004**, *120*, 10867−10870. (c) Xu, Q.-H.; Wang, S.; Korystov, D.; Mikhailovsky, A.; Bazan, G. C.; Moses, D.; Heeger, A. J. *Proc. Natl. Acad. Sci. U.S.A.* **2005**, *102*, 530−535.
(8) Lewis, F. D.; Wu, Y.; Zhang, L.; Zuo, X.; Hayes, R. T.; Wasielewski, M. R. *J. Am. Chem. Soc.* **2004**, *126*, 8206−8215.
(9) (a) Herrera, J. E.; Chaires, J. B. *Biochemistry* **1989**, *28*, 1993−2000. (b) Dickerson, R. E.; Goodsell, D. S.; Niedel, S. *Proc. Natl. Acad. Sci. U.S.A.* **1994**, *91*, 3579−3583.
(10) Lewis, F. D.; Wu, T.; Liu, X.; Letsinger, R. L.; Greenfield, S. R.; Miller, S. E.; Wasielewski, M. R. *J. Am. Chem. Soc.* **2000**, *122*, 2889−2902.
(11) (a) Champagne, B. B.; Pfanstiel, J. F.; Plusquellic, D. F.; Pratt, D. W.; Van Herpen, W. M.; Meerts, W. L. *J. Phys. Chem.* **1990**, *94*, 6−8. (b) Halasinski, T. M.; Weisman, J. L.; Ruiterkamp, R.; Lee, T. J.; Salama, F.; Head-Gordon, M. *J. Phys. Chem. A* **2003**, *107*, 3660−3669.
(12) Lewis, F. D.; Liu, X.; Wu, Y.; Miller, S. E.; Wasielewski, M. R.; Letsinger, R. L.; Sanishvili, R.; Joachimiak, A.; Tereshko, V.; Egli, M. *J. Am. Chem. Soc.* **1999**, *121*, 9905−9906.
(13) Wong, K. F.; Bagchi, B.; Rossky, P. J. *J. Phys. Chem. A* **2004**, *108*, 5752−5763.

JA0524402